NOVEL Ni-ZnCoFeAlLDH HETEROSTRUCTURES AND THEIR DERIVED MIXED OXIDES: STUDIES ON THE STRUCTURAL AND NANOMORPHOLOGY PROPERTIES

Eugenia Corina IGNAT[1], Gabriela CARJA[2]*

This study presents the synthesis and characterization of novel heterostructures obtained from the layered double hydroxide (LDH) of ZnCoFeAlLDH reconstructed in an aqueous solution of NiSO4·7H2O, along with their corresponding mixed oxides (MMOs) formed after calcination. The fabrication process is based on the LDH's ability to restore its layered structure, which is disrupted during calcination, demonstrating the 'structural memory effect.' Structural and morphological analyses were conducted using X-ray powder diffraction (XRD), coupled with scanning electron microscopy (SEM) and transmission electron microscopy (TEM-HRTEM/EDX). The findings reveal the formation of very small NiO nanoparticles on the plates of ZnCoFeAlLDH, showcasing the heterostructuring of the two nanounits.

Keywords: Layered double hydroxides, mixed metal oxides, nickel nanoparticle, structural memory effect

1. Introduction

LDH (layered double hydroxides) or hydrotalcites, included in the large family of anionic clay materials, are captivating inorganic layered materials with clearly defined 2D structure. The chemical composition of the LDH, expressed by the formula $[M^{II}_{1-x}M^{III}_{x}(OH)_2]^{x+}(A_{x/n})^{n-} \cdot mH_2O$, shows the positive charge of the metal hydroxide layers, caused by the partial isomorphous replacement of MII (Mg, Zn, Co, Ni, Ca, Fe, Cu, Cd) with MIII (Al, Ga, Cr, Fe) and the interlayer anions (organic or inorganic, Cl^-, SO_4^{2-}, NO_3^-, CO_3^{2-}, etc.), which balances, together with adsorbed water, the positive charge and attracts stability in the structure, [1]. The dispersion of different metal nanoparticles on the surface of LDH, that leads to significant improvement in the properties of Me-LDH heterostructures, can be achieved by the reconstruction. Furthermore, a notable characteristic of LDH consists in changing their structure after a calcination treatment, when the mixed MMO and spinels are formed. The original structure of

[1] PhD student, Faculty of Chemical Engineering and Environmental Protection, "Gheorghe Asachi" Technical University of Iaşi, Romania, e-mail: ignat.corina0702@gmail.com
[2]* Prof., Faculty of Chemical Engineering and Environmental Protection, "Gheorghe Asachi" Technical University of Iaşi, Romania, *corresponding author, e-mail: gcarja@ch.tuiasi.ro

the LDH can be restored in aqueous solutions containing anions. The calcination-reconstruction procedure defines the "memory effect" of LDH [2].

In our study, heterostructuring of Ni nanoparticles and LDH was achieved by exploiting the structural memory of ZnCoFeAlLDH in the aqueous solution of $NiSO_4 \cdot 7H_2O$. ZnCoFeAlLDH recovered its layered structure using SO_4^{2-} anions from the aqueous solution. Detailed investigation of the novel materials before and after calcination was carried out using XRD, SEM and TEM/EDX.

2. Experimental

2.1. Materials Preparation

The parent matrix, denoted as ZnCoFeAlLDH, was obtained following the coprecipitation technique, which involves mixing, by slowly adding, a $NaOH/Na_2CO_3$ solution under continuous stirring and the solution containing the appropriate amounts of metal salts (with M^{2+}/Me^{3+} molar ratios of 3/1), under rigorous verification and constant maintenance of the pH value at 8, respectively, the temperature (338 K). The resulting reddish suspensions were then placed in the ultrasound bath at 59 Hz and 333 K for 30-40 minutes and later aged for approximately 16 h at 338 K, recovered by vacuum filtration, washed twice with distilled water, and dried at 353 K in an oven for 6 h. All the chemicals $ZnSO_4 \cdot 7H_2O$, $CoSO_4 \cdot 7H_2O$, $FeSO_4 \cdot 7H_2O$, $Al(NO_3)_3 \cdot 9H_2O$, NaOH, and Na_2CO_3 were commercially available from Sigma Aldrich (99.9%), being used without further purification. 3 g of the obtained sample was calcined at 723 K for 5 h, and the resulting sample was then introduced into an aqueous solution of $NiSO_4 \cdot 7H_2O$ (99.9%, Sigma Aldrich). The resulting suspension was kept under solar irradiation using a solar light simulator (UNNASOL US800, 250 W) for 30 min, with slow stirring, in order to facilitate the rapid reconstruction of the original LDH. The sample thus obtained was separated by centrifugation and dried in an oven at 363 K. This sample was denoted as Ni-ZnCoFeAlLDH. Next, the precursor ZnCoFeAlLDH and the reconstructed LDH were calcined in air at 1173 K, for 5 h, and these samples were denoted as ZnCoFeAlLDH-c and Ni- ZnCoFeAlLDH-c, respectively.

2.2. Materials Characterization

Structural characteristics, phase formation, purity, and crystallinity information were examined using Bruker AXS D8 ADVANCE X-ray diffractometer in the Bragg–Brentano configuration, using the characteristic Kα radiation of copper ($\lambda = 0.15418$ nm), at a voltage of 40 kV and an intensity of 40 mA, within an angular range of $2\theta = (5 – 80)$ degree, speed 4 degrees/min, scan step: 0.02°. The analysis of the diffraction spectra was carried out by DIFFERENT EVE V.1.4 Evaluation software. The calculation of the structure constants corresponding to the rhombohedral symmetry was possible by applying

the relations a = 2d(110) and c = d(003), where the indices highlight the direction of the two characteristic planes found in the XRD diffraction pattern. DRIFT spectra measured by Nicolet 6700 FT-IR spectrometer using the standard KBr in the scanning range 400-4000 cm^{-1} and with averaging 200 scans. The spectral resolution was 4 cm^{-1}. The investigation of the particle morphology was carried out by collecting the data provided by the FEI Quanta FEG Scanning Electron Microscope (SEM) equipped with an X-ray detection system (EDX), which allows the precise determination of the chemical composition. TEM imaging was deciphered on a UHR-TEM LIBRA®200MC/Carl Zeiss GmbH ultra-resolution transmission electron microscope operating at 200 kV (acceleration voltage) together with the energy dispersive X-ray (EDX) spectrometer.

3. Results and Discussions

Fig. 1. shows the XRD patterns of ZnCoFeAlLDH and the reconstructed Ni-ZnCoFeAlLDH. The XRD pattern of ZnCoFeAlLDH indicates the formation of the hydrotalcite type phase, revealing the presence of the reflection peaks at 2θ = 11,824º, 23,625 º, 34,737 º, 39,422 º, 47,068 º, 60,281º, 61,547 º corresponding to (003), (006), (009), (015), (018), (110), and (113) diffraction planes, respectively [3]. In addition, in the XRD pattern of ZnCoFeAlLDH shows peaks of low intensity at 2θ = 34,2º (002) and 36,267º (101), that could be assigned to the formation of low crystalized ZnO phase.

The symmetrical and rather sharp basal reflections of planes (003), (006) and (009), observed in the XRD pattern of Ni-ZnCoFeAlLDH, demonstrate the complete restoration of the layered structure of LDH after the reconstruction in the $NiSO_4$ aqueous solution, despite the fact that the plane reflections non-basal (015) and (018) are of lower intensity and much wider. This suggests that for the heterostructured LDH, the size and crystallinity of the particles decreased [3].

Furthermore, there is a slight decrease, after the reconstruction, of the value of angle 2θ (from 11,824º for ZnCoFeAlLDH to 11,780º for Ni-ZnCoFeAlLDH) corresponding to the (003) plane, as a result of the expansion of the LDH structure by intercalation of the sulfate anion in the interlayers.

For the reconstructed Ni-ZnCoFeAlLDH no peaks due to the nickel phase were identified because the amount of Ni was below 5% or the size of Ni nanoparticles was very small, such as Ni phases could not be detected by XRD analysis.

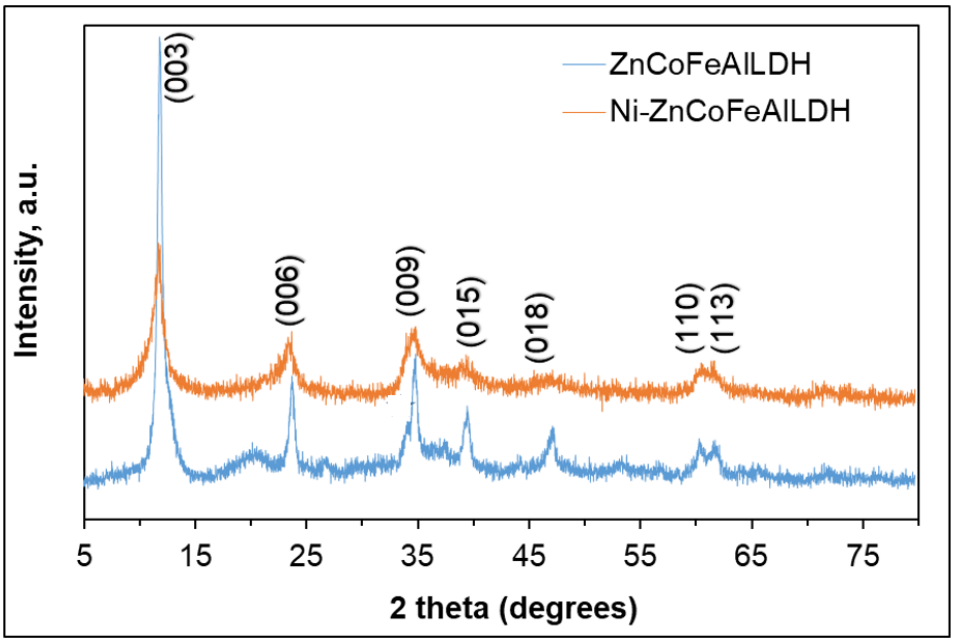

Fig. 1 − XRD patterns of ZnCoFeAlLDH and Ni-ZnCoFeAlLDH.

The difference observed in Fig. 1 for FWHM (full width at half the maximum) of the characteristic diffraction peaks of LDH corresponding to the matrix and the reconstructed sample implies a difference in the size of the crystallites calculated with the Scherrer equation (Eq.1) [4]:

$$D = \frac{k\,\lambda}{\beta\,\cos\theta} \tag{1}$$

where D is the crystallite size, K is the Scherrer constant, λ is the X-ray wavelength, and β is the FWHM).

From table 1, it is observed that the size of the crystallites is smaller for the Ni-ZnCoFeAlLDH heterostructures compared to the parent, which also reveals a decrease in the degree of crystallinity.

The values in Table 1 show that, after the reconstruction, the new LDH heterostructures do not reveal significant changes of the basal space and the interlamellar distance compared to the original LDH; this is explained by the fact that the sulfate anions intercalated in the LDH galleries already existed.

In the investigation of the LDH structure, another essential step is to determine the values corresponding to the parameters of the unit cells (Table 2).

The value of the parameter "*a"*, correlated with the average distance between the cations in the brucite-like layer, is slightly smaller for the reconstructed sample, which derives from the fact that the ionic radius of Ni (0.700 Å) is shorter compared to that of Co(II) (0.735 Å) and Zn (0.745 Å) [5].

Table 1

Peak positions for the (hkl) planes and the calculated interlayer distance (d) and crystallite sizes of samples

hkl	Sample name					
	ZnCoFeAlLDH			Ni-ZnCoFeAlLDH		
	2Θ, °	d, Å	D, nm	2Θ, °	d, Å	D, nm
003	11,824	7,484	18,051	11,780	7,512	12,889
006	23,625	3,765	19,620	23,630	3,762	9.088
009	34,737	2,580	18,292	34,325	2,610	8,011
015	39,422	2,283	22,079	39,322	2,289	9,36
018	47,068	1,929	12,62	45,421	1,995	5,450
110	60,281	1,535	24,035	60,499	1,530	20,371
113	61,547	1,505	57,121	61,375	1,509	53,166

Table 2

Crystal lattice parameters

Crystal lattice parameters	Calculation formula	Sample name	
		ZnCoFeAlLDH	Ni-ZnCoFeAlLDH
a, Å	2 d_{110}	3.07	3,06
c, Å	3 d_{003}	22,453	22,537
IFS, Å	d_{003} – 4,8 Å	2,684	2,712

Assuming the value of 4.8 Å as the width of the brucite-like layer, the calculated interlayer space (IFS) was 2,712 Å for Ni-ZnCoFeAlLDH in agreement with the locations of the sulfate anions.

From the X-ray patterns of the materials calcined at 1173,15 K, shown in Fig.2, it can be seen that the reflections corresponding to LDH disappeared and new strong reflections appeared. Thus, the peaks associated with the ZnO phase are centered at 2θ = 31.778° (100), 34.434° (002), 36.265° (101), 47.556° (102), 56.613° (110), 62.880° (103), 67.972° (112), 69.110° (201), 72.595° (004), and 76.988° (202) [6]. Further, the reflections at 36,46° correspond to the nickel aluminate $NiAl_2O_4$ (311) plane [7, 8, 9], while the peaks at 55,6° (422) and 77,43° can be due to the (422) and (622) planes of $ZnAl_2O_4$ [10]. In the XRD pattern Ni-ZnCoFeAlLDH-c, new phases of $FeCoZnAlO_4$ are found at 18,79° (111), 30,96° (220), 38.129° (222), 58,7° (511), 64,5° (440), and 76,4° (533).

The crystallite size for calcined samples was calculated considering the basal reflections (101) for the ZnO phase, (311) for the $NiAl_2O_4$ phase, (422) for

the $ZnAl_2O_4$ phase, and (511) for the $FeCoZnAlO_4$ phase using the Scherrer equation [4], and the results are presented in Table 3.

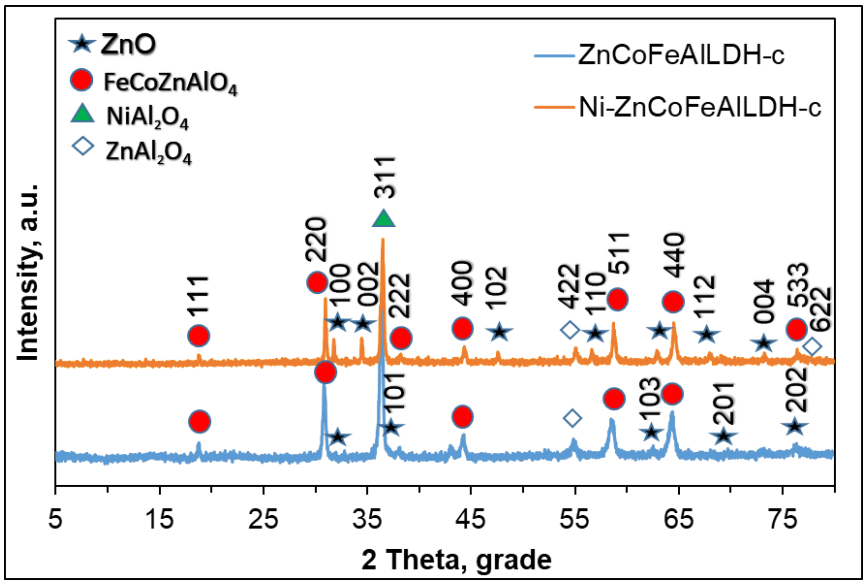

Fig. 2 − XRD patterns of ZnCoFeAlLDH-c and Ni-ZnCoFeAlLDH-c after calcination at 1173 K.

Table 3

The crystallite size for calcined samples

Phase MMO	Sample name					
	ZnCoFeAlLDH-c			Ni-ZnCoFeAlLDH-c		
	d, Å	FWHM, ^{0}	D, nm	d, Å	FWHM, ^{0}	D, nm
ZnO	2,475	0,281	33,080	2,475	0,224	41,498
$NiAl_2O_4$	-	-	-	2,461	0,223	41,710
$ZnAl_2O_4$	1,667	0,257	38,756	1,666	0,263	37,881
$FeCoZnAlO_4$	1,572	0,305	33,225	1,570	0,285	35,566

The FTIR spectra of the as-synthesized and calcined materials are shown in Fig. 3. The Ni-ZnCoFeAlLDH spectrum displays a strong band in the 3550–3200 cm^{-1} range, assigned to the O–H stretching vibrations. while the band at 1620 cm^{-1} is due to the bending vibrations of water molecules or hydroxyl groups. Further, the absorption bands at 1124 cm^{-1}, 1072 cm^{-1} and 964 cm^{-1} are likely associated with the asymmetrical and symmetrical bending vibrations of sulfate anions, corresponding to the ν_3, ν_2, and ν_1 modes, respectively. The vibration bands in the region of low wavenumbers (<700 cm^{-1}) point out the stretching of M-O, M-O-H and M-O-M [11]. For Ni-ZnCoFeAlLDH-c Fig.3 shows the significant modification of the interlayers due to the calcination. It is observed that the bands corresponding to $\nu_{O\text{-}H}$ and δH_2O disappears upon calcination at

1173 K due to the destruction of the metal hydroxide layers of LDH and the removal of water molecules from the interlayers.

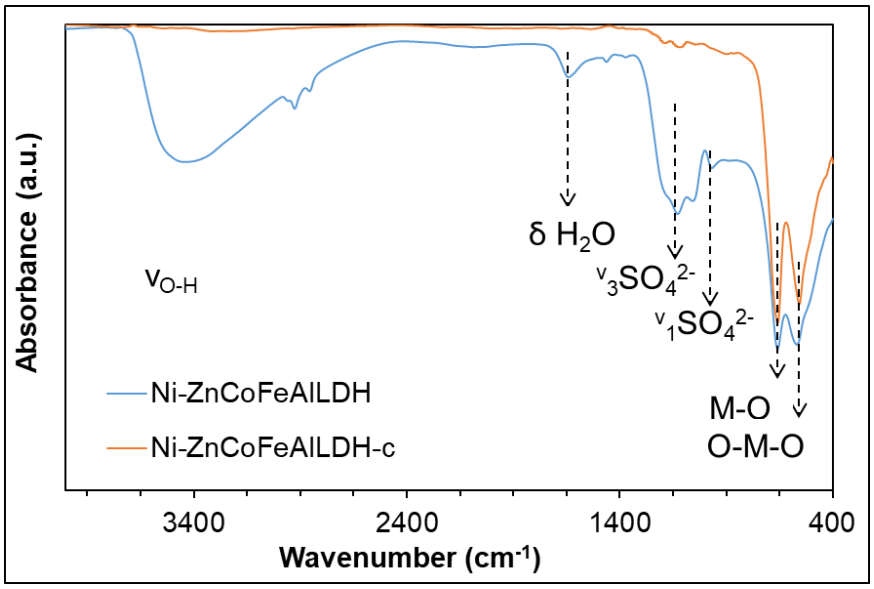

Fig. 3 – FTIR spectra of Ni-ZnCoFeAlLDH and Ni-ZnCoFeAlLDH-c.

The textural characteristics, respectively. of the chemical composition of Ni-ZnCoFeAlLDH and Ni-ZnCoFeAlLDH–c was analyzed using the SEM-EDX technique, with the images recorded for the samples before and after calcination being illustrated in Fig. 4.

The similar morphology of the two samples can be observed, showing the porous structure of the sponge. More irregularly aggregated particles without typical platelets can also be observed; the structure of the rough surface with particles of different shapes is preserved after calcination.

Similarly, the EDX of the prepared Ni-ZnCoFeAlLDH and Ni-ZnCoFeAlLDH-c indicate the successful incorporation of Ni in the LDH.

The investigation of the nature and quantitative presence of the chemical species was carried out using energy dispersive X-ray spectroscopy (EDX).

The EDX spectra of the reconstructed samples, before and after calcination (see Fig. 4), together with the results presented in the Table 4, highlight the predominant presence of the elements Zn, Co, Fe, Al, and Ni.

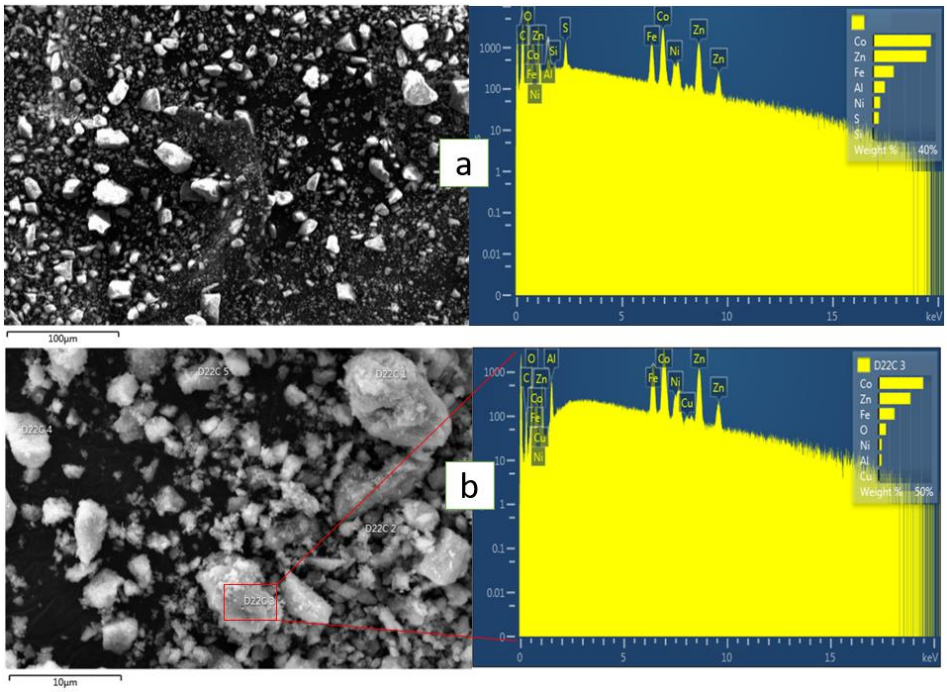

Fig. 4 − The SEM pictures and corresponding EDX spectra of Ni-ZnCoFeAlLDH (a) and Ni-ZnCoFeAlLDH – c (b).

Table 4

The chemical composition of Ni_ZnCoFeAlLDH and Ni_ZnCoFeAlLDH – c

Sample	Compoziția chimică (wt%)[x]				
	Zn	Co	Fe	Al	Ni
Ni-ZnCoFeAlLDH	34,0	36,9	13,2	7,5	4,6
Ni-ZnCoFeAlLDH - c	37,28	38,24	13,5	6,44	3,98

[x] The arithmetic mean of the results obtained based on quantitative EDX data

Moreover, the EDX spectra clearly indicates the existence of characteristic peaks for Ni, thus confirming the formation of heterostructuring of the quaternary LDH coupled with nickel nanoparticles.

Based on the EDX results (Table 3), relatively small amounts of Ni (< 5 wt%) were detected on the surface. This small amount justifies the absence of the typical reflections of Ni phases from the corresponding XRD diffractograms.

The investigation of the nanomorphology of the reconstructed Ni-ZnCoFeAlLDH was analyzed by TEM and HRTEM and the results are given in Fig. 5. It clearly reveals the formation of very small Ni nanoparticles, with an average diameter lower as 10 nm dispersed on the nanoplates of ZnCoFeAlLDH. Next, the image in Fig. 5e reveals the SAED pattern indicating the fringe corresponding to well crystallized NiO, thus confirming the heterostructuring.

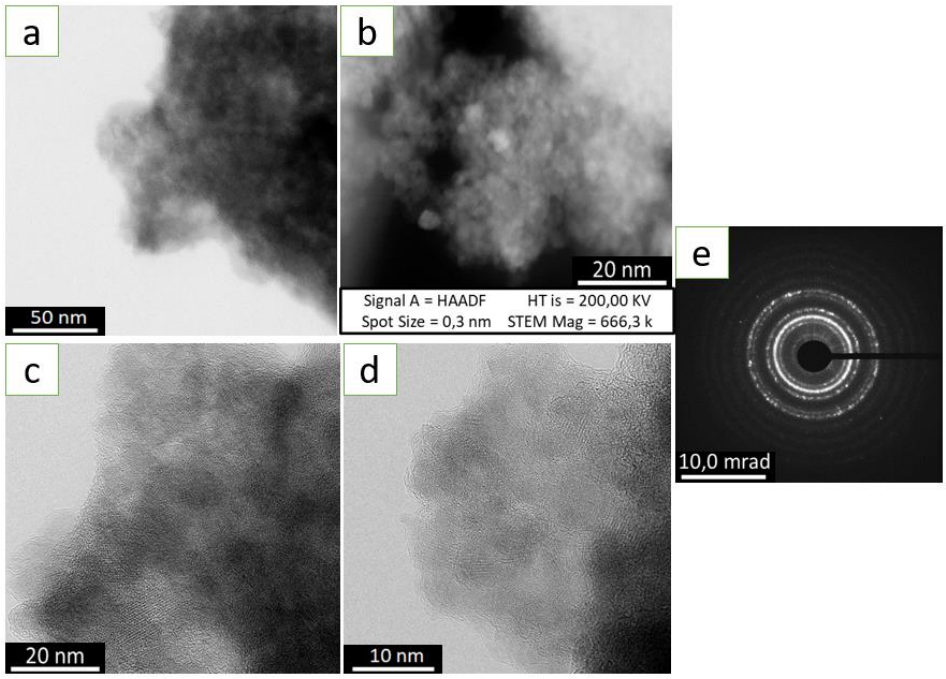

Fig. 5 − (a) TEM image, (b) STEM image, (c, d) HRTEM image, and (e) SAED image of Ni-ZnCoFeAlLDH

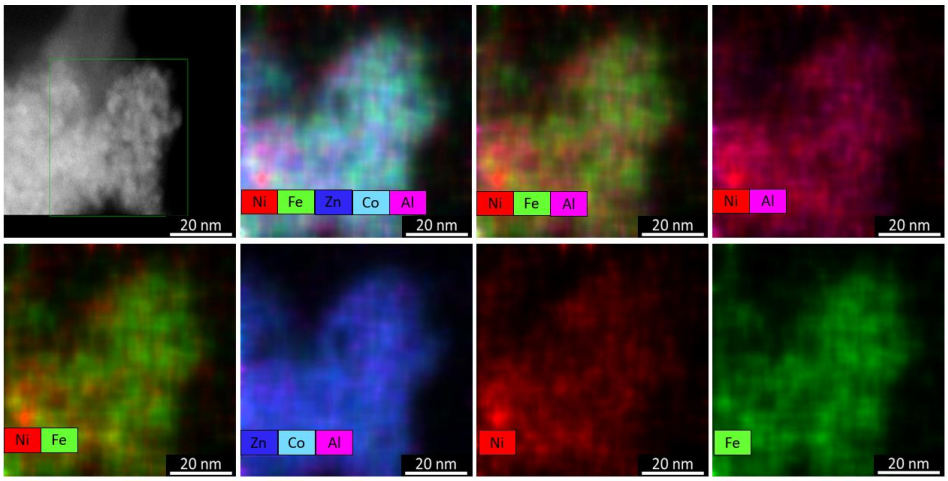

Fig. 6 − EDX mapping of Ni-ZnCoFeAlLDH

Elementary mappings in Fig. 6 confirm the presence of Ni, Zn, Co, Fe, and Al in Ni-ZnCoFeAlLDH, indicating the successful heterostructuring between nanoparticles of Ni and ZnCoFeAlLDH. Consequently, the EDX-TEM results align with the findings from EDX-SEM.

4. Conclusions

Heterostructuring of small Ni nanoparticles (average diameter lower than 10 nm) and ZnCoFeAlLDH was successfully achieved by exploiting the reconstruction process by "memory effect" of ZnCoFeAlLDH in an aqueous solution of $NiSO_4$. Homogeneous mixtures of mixed oxides were obtained after calcination at 723 K. The results can pave the way to develop novel materials as complex heterostructures for advanced applications in catalysis and nanotechnology.

R E F E R E N C E S

[1]. *S. Li, W. Dongdong, X. Wu, Y. Chen,* Recent advance on VOCs oxidation over layered double hydroxides derived mixed metal oxides, Chinese Journal of Catalysis, **41**(4), 2020, 550-560.

[2]. *D. Kwon, J.Y. Kang, S. An, I. Yang, J.C. Jung,* Tuning the base properties of Mg–Al hydrotalcite catalysts using their memory effect, Journal of Energy Chemistry **46**, 2020, 229–236.

[3]. *G. Carja, E.F. Grosu, M. Mureseanu, D. Lutic,* A family of solar light responsive photocatalysts obtained using $Zn^{2+}Me^{3+}$ (Me = Al/Ga) LDHs doped with Ga_2O_3 and In_2O_3 and their derived mixed oxides: a case study of phenol/4-nitrophenol decomposition, Catal. Sci. Technol., **7**(22), 2017, 5402–5412.

[4]. *L. Santamaria, L. Oliveira García, E.H. de Faria, K.J. Ciuffi, M.A. Vicente, S.A. Korili, A. Gil,* M(II)- Al-Fe layered double hydroxides synthesized from aluminum saline slag wastes and catalytic performance on cyclooctene oxidation, Minerals Engineering **180**, 2022, 107516.

[5]. *W. Gou, X. Mo, C. Ren, H. Wang, W. Li,* Formation of crystalline multimetallic layered double hydroxide precipitates during uptake of Co, Ni, and Zn onto γ-alumina: Evidence from EXAFS, XRD, and TEM, Chemosphere **307**, 2022, 136055.

[6]. *R. Mahmoud, H.F.M. Mohamed, S.H.M. Hafez, Y.M. Gadelhak, E.E. Abdel-Hady,* Valorization of spent double substituted Co–Ni–Zn–Fe LDH wastewater nanoadsorbent as methanol electro-oxidation catalyst, Scientifc Reports, **12**(1), 2022, 19354.

[7]. *T. Rajkumar, A. Sápi, M. Ábel, F. Farkas, J.F. Gómez-Pérez, Á Kukovecz, Z. Kónya,* Ni–Zn–Al-Based Oxide/Spinel Nanostructures for High Performance, Methane-Selective CO_2 Hydrogenation Reactions, Catalysis Letters, **150**, 2020, 1527–1536.

[8]. *F. Rahbar Shamskar, M. Rezaei, F. Meshkani,* The influence of Ni loading on the activity and coke formation of ultrasoundassisted co-precipitated Ni–Al2O3 nanocatalyst in dry reforming of methane, Int. J. Hydrogen Energy, **42**, 2017, 4155–4164.

[9]. *K.H. Song, S.K. Jeong, B.H. Jeong, K.Y. Lee, J. Kim,* Effect of the Ni/Al Ratio on the Performance of $NiAl_2O_4$ Spinel-Based Catalysts for Supercritical Methylcyclohexane Catalytic Cracking, Catalysts, **11**(3), 2021, 323.

[10]. *X. Yuan, Q. Jing, J. Chen, L. Li,* Photocatalytic Cr(VI) reduction by mixed metal oxide derived from ZnAl layered double hydroxide, Appl. Clay Sci. **143**, 2017, 168–174.

[11]. *A.R. Sotiles, N.A.G. Gomez, M.P. dos Santos, M.T. Grassi, F. Wypych,* Synthesis, characterization, thermal behavior and exchange reactions of new phases of layered double hydroxides with the chemical composition $[M_6^{+2}Al_3(OH)_{18}(SO_4)_2].(A(H_2O)_6).6H_2O$ (M^{+2} = Co, Ni; A = Li^+, Na^+, K^+), Appl. Clay Sci. **181**, 2019, 105217.